DYNAMIC ANALYSIS AND BALANCING OF AN 1150 MW TURBINE-GENERATOR SYSTEM

by

E. J. Gunter
Department of Mechanical, Aerospace and Nuclear Engineering
University of Virginia
Charlottesville, VA

J. R. Henderson
San Onofre Nuclear Generating Station
San Clemente, CA

W. E. Gunter
RODYN Vibration Analysis, Inc.
Charlottesville, VA

Edgar Gunter is a Professor of Mechanical and Aerospace Engineering at the University of Virginia. He received a Ph.D. degree in Engineering Mechanics in 1965 from the University of Pennsylvania. He has worked in the field of vibrations of rotating machinery and fluid bearings for over 30 years and has written over 150 technical papers and reports on various aspects of the dynamics of rotating machinery, fluid film bearings and balancing. For the past 8 years, he has been working extensively with finite element analysis of rotating machinery on the microcomputer. He has had extensive experience with the dynamic analysis and balancing of both steam and gas turbine generators. Dr. Gunter has worked with utilities on various problems connected with high-pressure seal injection pumps, turbine-generators and fans.

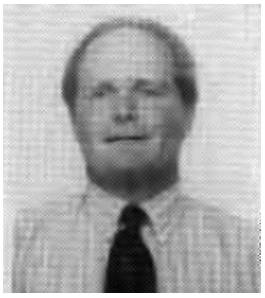

Jim Henderson is an engineer for the Southern California Edison Co. at the San Onofre Nuclear Generating Station (SONGS) in San Clemente, California. He has been dynamically monitoring the 1150 MW SONGS turbine-generators since 1983. He was involved with the initial field balancing operations following the Unit 3 Commercial Run, and has performed single- and multi-plane trim balance shots.

Jim designed the customized shaft absolute vibration monitoring system using Bently dual probes and XY vibration monitors on the turbines, and also directed the SCE specification and procurement of the first hard bearing, transportable 250-ton-slow speed rotor balance machine sold by Schenck-Treble.

William Gunter is an engineer at RODYN Vibration Analysis, Inc. He received a BSEE degree from the University of Virginia (1979). Bill has previously worked at United Technologies as an Electrical Engineer with an emphasis on computer simulation of analog electronics. He is now performing FEA modeling and computer simulation of rotor dynamic systems at RODYN.

ABSTRACT

Large turbine-generators have proven to be very difficult to field balance with the application of weights at only single or two planes. This paper presents a method of multi-plane balancing based on actual measured system influence coefficients and theoretically derived coefficients for an 1150 MW turbine-generator system. This class of turbine-generator cannot be balanced by the repeated application of single- or two-plane balancing. A simultaneous, multi-plane balancing procedure such as the method outlined in this paper is required.

1 INTRODUCTION

This paper presents the dynamic analysis for a large 1150 MW 11-bearing nuclear turbine-generator system, which weighs approximately 1.6 million lb (727,300 Kg) and is 2,427 in (61.65 M) long. It is composed of a high-pressure turbine, three low-pressure turbines, a generator and an exciter, which is one of the largest nuclear turbine-generator units in the world. The system has a normal operating speed of 1,800 RPM. A previous paper was presented on the static deflection, characteristic bearing loads, and bearing stiffness and damping characteristics for the turbine-generator. The objective of the study was to understand the dynamical characteristics of the entire turbine-generator system in order to better understand and facilitate the field balancing process. It was also desirable to determine whether initial component balancing of the turbines and generator would facilitate field balancing.

2 CRITICAL SPEEDS OF INDIVIDUAL TURBINE-GENERATOR COMPONENTS

As the first step in analyzing the dynamic characteristics of the 1150 MW turbine-generator set, the critical speeds and mode shapes were generated for each component of the system. The major components of the turbine-generator set consist of a high pressure turbine (HP) and three low pressure turbines connected to a generator, which in turn has an exciter attached.

2.1 High Pressure Turbine

Figure 1, for example, represents the first mode for the HP turbine. The turbines and generator were analyzed using the transfer matrix program ***CRITSPD-PC***. The HP turbine is approximately 380 in. (31.7 ft.) long and weighs over 150,000 lb (75 tons). For an assumed bearing stiffness of K_b= 4,0E6 lb/in, Figure 1 shows the first HP turbine critical speed to be approximately 1,200 RPM (120 Hz).

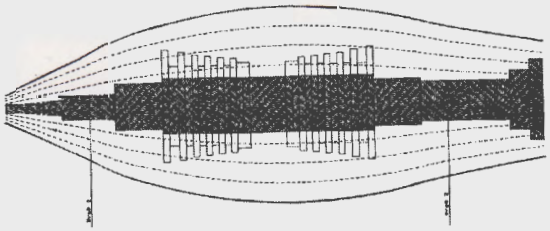

Figure 1 - High Pressure Turbine 1st Critical Speed with K_b = 4.0E6 lb/in N1 = 1,200 RPM (20 Hz)

A reduced mass station model was next generated to match the original model's first three critical speeds. This step is necessary in the construction of the entire system model from the individual components.

Figure 2 represents the HP turbine second critical speed predicted to be 1,710 RPM (28.5 Hz).

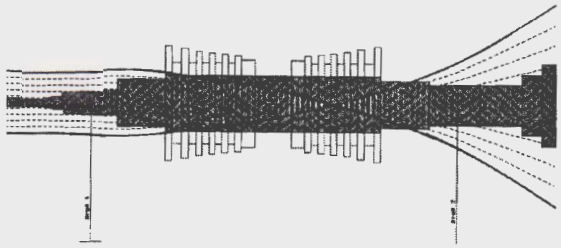

Figure 2 - High Pressure Turbine 2nd Critical Speed with K_b = 4.0E6 lb/in N2 = 1,710 RPM (28.5 Hz)

This value is very close to the operating speed of 1,800 RPM (30.0 Hz). Note that the coupling on the right end is attached to the first low pressure turbine. Since the coupling has considerable amplitude and slope, this mode will be influenced by the stiffness of the adjacent low pressure turbine.

2.2 Low Pressure Turbine

There are three low pressure turbines attached to the right of the high pressure turbine. These turbines will be referred to as LP1, LP2, and LP3. The coupling connecting the HP turbine to LP1 will be referred to as C1 and the coupling connecting LP1 to LP2 will be referred to as C2. Coupling C3 connects LP2 to LP3. The LP turbines are approximately 425 in. long (35.4 feet) and weigh 340,000 lb (170 tons) each. The low pressure turbines are larger and have over twice the weight of the high pressure turbine. Therefore, the low pressure turbine first critical speed is lower. Figure 3 indicates that the third critical speed is 1,890 RPM (31.5 Hz) with an assumed bearing stiffness of 2.0E6 lb/in. The operating speed of 1,800 RPM is above the predicted second critical speed for the LP turbines. After the completion of the detached LP rotor model, a reduced LP model was generated with only one-half of the stations of the original LP model.

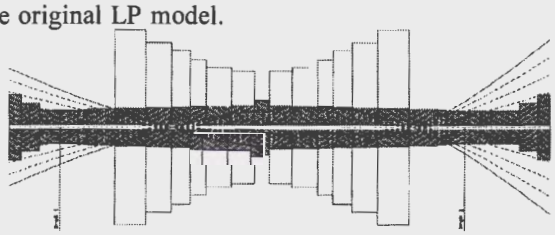

Figure 3 - Low Pressure Turbine 3rd Mode at 1,890 RPM (31.5 Hz) with K_b = 2.0E6 lb/in

2.3 Generator

The generator is over 651 in long (54 feet) and weighs over 428,999 lb (214 tons). Since the generator has the longest span of any of the components and is the heaviest, it has the lowest first critical speed. Figure 4 represents the generator mode shape for the third critical speed at 2,062 RPM (34.4 Hz) for an assumed value of bearing stiffness of 2E6 lb/in.

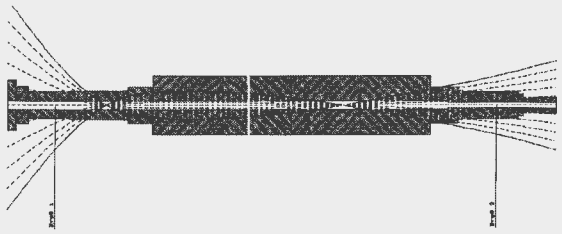

Figure 4 - Generator 3rd Critical Speed with K_b = 2E6 lb/in N3 = 2,062 RPM (34.4 Hz)

Figure 5 represents the first four generator critical speeds as a function of bearing stiffness. At a high bearing stiffness of K_b = 7.0E6 lb/in, the generator second critical speed will be at the operating speed. The operating speed on Figure 5 is shown as a dot-dash line.

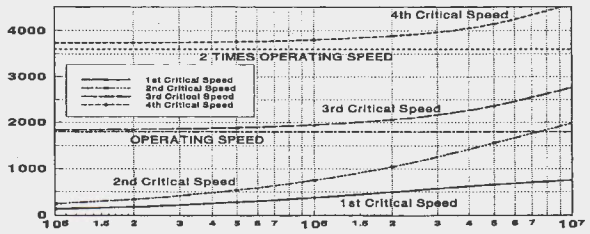

Figure 5 - Critical Speeds of Generator as a Function of Bearing Stiffness

It is seen that the generator would be operating above the second critical speed for bearing stiffnesses less than 6E6 lb/in. The third critical speed is above the operating speed. The plot of the fourth critical speed is also shown on this figure. It is not desirable to have the rotor fourth critical speed to be exactly twice the operating speed. It is also undesirable to have a generator critical speed at exactly 60 Hz. Electrical line faults will cause 120 Hz excitation in a generator, which can excite the higher order torsional-lateral modes. The 120 Hz excitation has caused LP3 torsional blade vibration and subsequent blade loss in other nuclear turbine-generators.

2.4 Generator-Exciter

The generator was combined with the exciter to determine the combined generator-exciter modes. Figure 6, for example, represents an exciter mode at 1,452 RPM (24.2 Hz). This mode can be excited by unbalance at the exciter or by suddenly applied unbalance at the LP3 turbine due to blade loss.

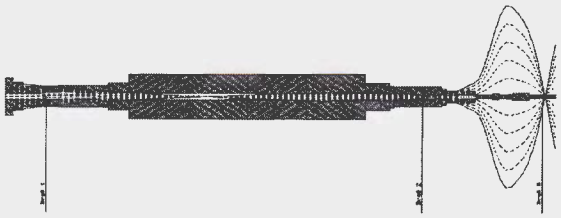

Figure 6 - Exciter-Generator Critical Speed at 1,452 RPM (24.2 Hz)

There is no monitoring probe between the outboard generator and the exciter bearing to monitor the exciter behavior. This mode shows the importance of placing a vibration pickup between the 10th (generator outboard) and 11th bearings (exciter) to monitor exciter motion.

3 Turbine-Generator System Critical Speeds

It was determined that there are only minor gyroscopic effects involved with the turbines or the generator at or below 1,800 RPM. Finite element models were generated for each component which matched the transfer matrix models. The finite element method of analysis is preferred to the transfer matrix method for large turbine-generators. The finite element method has the distinct advantage over the transfer matrix method in that it does not miss modes that are closely spaced. In addition, it has fewer numerical convergence problems, particularly when flexible foundations with mass are included in the model. The finite element program ***MSC/Pal*** was employed for the calculation of the natural frequencies.

The finite element model was also used to determine the static deflected mode shape of the system, as well as the combined dynamical modes of motion. Also, the finite element model could be used to determine the system forced response with unbalance and bearing stiffness and damping.

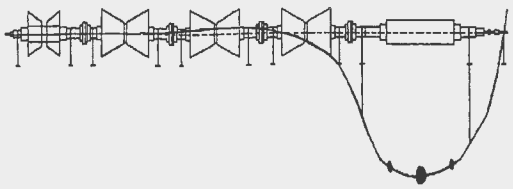

Figure 7 - First Turbine-Generator Mode Generator First Mode at 496 RPM

The first five modes of the system involve the component mass center of the generator and the various turbines. The first system critical speed is shown in Figure 7 at 496 RPM. This mode is the generator first critical speed, as would be expected, since it is the longest and heaviest of the components. Its natural frequency is relatively unaffected by the LP3 turbine. This mode is driven by unbalance at the generator mass center. This mode can be corrected by low speed balancing of the generator on a balancing machine. Center span unbalance can also occur during operation due to the thermal effects of the generator electrical conductors, which can cause shaft bowing.

The next three turbine-generator modes involve the mass centers of the LP turbines. These modes occur within a narrow range of each other. When using the transfer matrix method to compute these modes, several modes were initially missed due to the frequency marching method and step increment used in the transfer matrix procedure. A great advantage of the finite element method is that it does not skip or miss modes. In Figure 8, which is the turbine-generator system second mode at 562 RPM, the motion of the three mass centers is in phase.

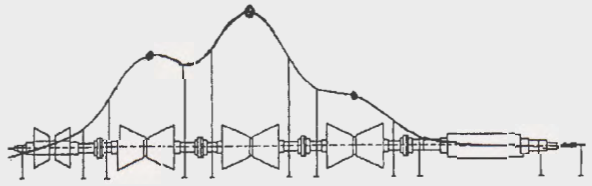

Figure 8 - 2nd Turbine-Generator Mode LP Rotors in Phase at 562 RPM

Figure 9 represents the third turbine-generator mode at 569 RPM. In this mode, the mass center of LP1 is out of phase to the mass center of LP3. The second and third system modes would be well controlled by the rigid rotor balancing of the LP rotors. Coupling alignment would have little influence on this mode.

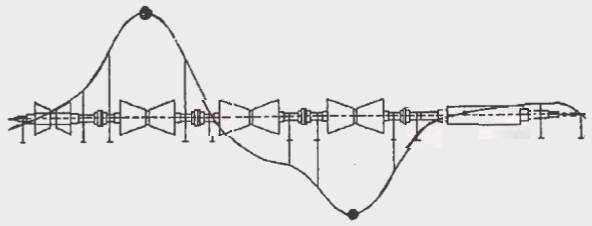

Figure 9 - 3rd Turbine-Generator Mode LP1 and LP3 out of Phase (569 RPM)

The fourth turbine-generator mode at 585 RPM, as shown in Figure 10, shows that the LP1 and LP3 turbines are moving out of phase to the LP2 turbine. These three modes are similar to the behavior of a large three-mass rotor model.

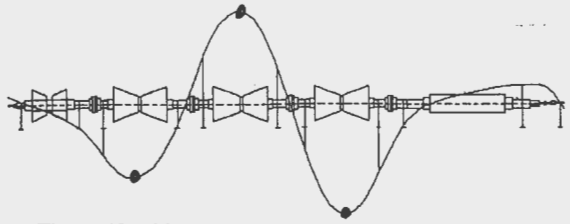

Figure 10 - 4th Turbine-Generator Mode - LP2 Out of Phase to LP1 and LP3 (585 RPM)

The fifth system turbine-generator critical is identical to Figure 1 for the high pressure turbine at 1,182 RPM. The mode shape and first critical speed of the HP turbine is relatively unaffected by the LP turbines.

Figures 11 and 12 represent the turbine-generator sixth and seventh modes at 1,037 RPM and 1,162 RPM. These two modes are bifurcated modes of the generator second critical speed interacting with the turbines. The sixth mode at 1,037 RPM, as shown in Figure 11, corresponds with the original turbine-generator second critical speed.

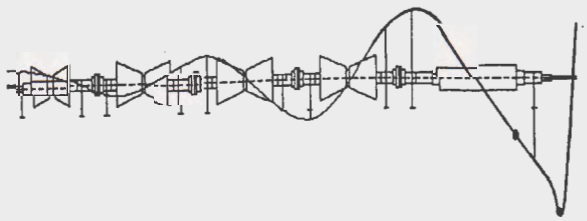

Figure 11 - 6th Turbine-Generator Mode Generator Second Mode (1,037 RPM)

In Figure 12, the slightly higher speed of the seventh mode (1,162 RPM) is caused by the interaction of the LP1 and LP2 turbines with the generator. Modes six and seven would probably appear as a single mode in the experimental test data. Note that unbalance at the No. 2 coupling C2 can have a strong effect on this mode.

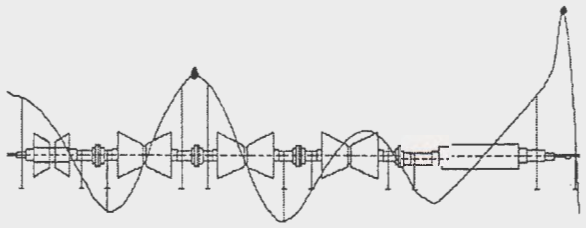

Figure 12 - 7th Turbine-Generator Mode Generator 2nd Mode with LP Turbines (1,162 RPM)

Figure 13 is the ninth turbine-generator mode at 1,459 RPM and is essentially the exciter first mode. If there is no monitoring station between the 10th and 11th bearings, the exciter mode will not be observed. Also, blade loss at LP3 could cause a violent transient excitation of the turbine-generator eighth mode, with large exciter amplitude.

Figure 13 - 9th Turbine-Generator Mode Exciter 1st Mode (1,459 RPM)

Figure 14 represents the 10th mode of the turbine-generator system at 1,673 RPM. Depending upon the assumptions of bearing stiffnesses, the 10th mode may be even closer to the operating speed at 1,800 RPM. This mode is of considerable importance from the standpoint of understanding multi-plane balancing of the turbine-generator.

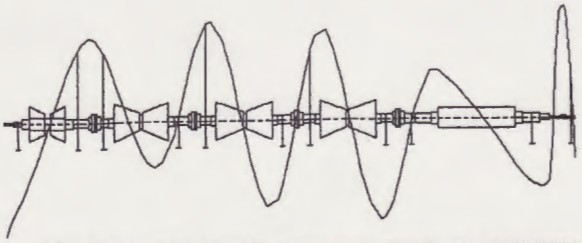

Figure 14 - 10th Turbine-Generator Mode at 1,673 RPM

After passing through the first five critical speeds, the turbine and generator mass centers became node points. This means that there is very little motion at the mass centers of the turbines or the generators. Figure 14 shows that there are 10 node points along the axis of the turbine-generator for the 10th mode. Theoretically, a minimum of 10 planes of balancing would be required to balance all 10 modes. Although coupling No. 1 between the HP and LP1 turbines has not been used as a balancing plane, Figure 14 shows that the first coupling location will have a considerable influence along the entire length of the turbine-generator.

Table 1 represents the calculations of the critical speeds for the turbine-generator set using the transfer matrix ***CRITSPD-PC*** program and the finite element program ***MSC/Pal2*** (now superseded by ***CDA/sprint***). The difference between the critical speeds predicted by both methods is less than 1%, except for mode six, which is 1.5%. An advantage of the finite element method is that the iteration procedure does not miss modes, which can happen with the transfer matrix method. The transfer matrix method is advantageous for the initial development of the component models and also for the development of the effective reduced station rotors which are used in the final assembly. However, for large turbine-generator with foundation effects, the finite element method is the preferred approach.

Critical Speeds of SONGS Turbine-Generator System

W_{total} = 1,597,789 lb 11 Bearings
K_{brg} = 2.0E6 lb/in

	TMM (RPM)	FEM (RPM)	Δ (RPM)	%
1	511	512	+ 1	0.2
2	582	584	+ 2	0.3
3	586	588	+ 2	0.3
4	596	598	+ 2	0.3
5	934	937	+ 3	0.3
6	1,060	1,076	+16	1.5
7	1,187	1,195	+ 8	0.7
8	1,378	1,388	+10	0.7
9	1,491	1,504	+13	0.9
10	1,674	1,691	+17	1.0

TMM — Transfer Matrix Method — *CRITSPD-PC*
FEM — Finite Element Method — *MSC/PAL2*

Table 1 - Comparison of Critical Speeds Using Transfer Matrix and Finite Element Methods

4 Influence Coefficients and Multi-Plane Balancing of Turbine-Generator

From the evaluation of the theoretical turbine-generator system critical speeds, much useful information on the balancing procedure for the 11-bearing turbine-generator is obtained. To perform an actual multi-plane balance run, influence coefficients of the turbine-generator to various balancing planes must be first experimentally determined. It is desirable to be able to balance the turbine-generator by the application of weights at the couplings and at the ends of the LP turbines. It is not practical to apply field balance weights to the generator because of its operation in a hydrogen environment.

4.1 Theoretical Coupling No. 1 Influence Coefficients

From the observation of Figure 14 of the system 10th mode, it can be seen that the first coupling location would provide an excellent balancing plane for trim balancing the turbine-generator at speed. In practice, however, only the second, third, and fourth coupling locations have been used. The influence coefficients for the first coupling, referred to as location C1, were generated analytically from the finite element program. A forcing function was placed at coupling location 1 and the forced response, including bearing damping, was computed for 1,800 RPM. Figure 15 represents the response of the rotor due to an unbalance force placed at the first coupling. The rotor response is a three-dimensional space curve because of the influence of bearing damping.

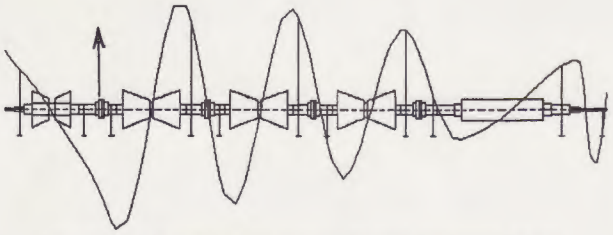

Figure 15 - Turbine-Generator Forced Response Mode Shape with Coupling No. 1 Unbalance at 1,800 RPM

Figure 16 represents the in-plane and out-of-plane components of the response to unbalance at the No. 1 coupling. If there is no system or bearing damping, then the out-of-plane amplitude represented by the dotted line would be zero. For example, at the critical speed for a

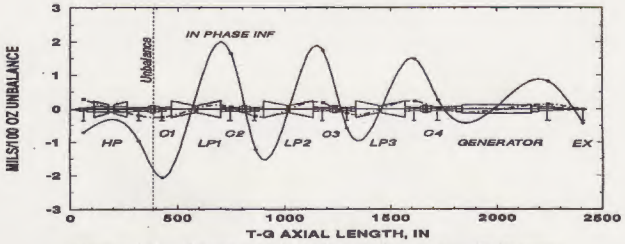

Figure 16 - Theoretical Turbine-Generator Influence Coefficients at 1,800 RPM Due to Coupling No. 1 Unbalance

single mass model, the out-of-plane response is lagging the forcing function by 90°. The in-plane and out-of-plane components of the influence coefficients are computed by multiplying the influence coefficient amplitude by the cosine or sine of the relative phase angle response to the unbalance vector.

In the actual system, measurements are made only at the 11 bearings. Figure 16 was generated by using only 11 amplitude and phase values computed for the bearings. A cubic spline curve fit was used to connect the points. The cubic spline curve fit identically matches beam theory. Thus, by using a cubic spline curve fit to only the bearing amplitudes, the amplitude at other sections may be accurately predicted, except at the exciter-generator region.

Note that the cubic spline curves pass through the mass centers of the LP turbines and the generator. By comparing Figures 15 and 16, it can be seen that the cubic spline curve fit does not match the shape of the rotor motion in the vicinity of the generator and exciter. To produce a more accurate curve in this vicinity, a measurement must be taken between the 10th and 11th bearings. Therefore, it is important to have a probe monitor the exciter motion when placing balancing weights along the shaft.

4.2 Experimental Coupling Influence Coefficients

Experimental coupling influence coefficients have been obtained for weights placed on couplings 2, 3, and 4. The influence coefficients for a particular coupling location are obtained by subtracting the rotor response before and after the application of a trial weight and normalizing by the trial weight. Figure 17 represents the experimental turbine-generator response due to a weight placed at the No. 2 coupling between the LP1 and LP2 turbines. The response is given in terms of mils per 100 oz of applied unbalance at a 19.9 in. radius. Note that the C2 coupling shot causes a 90° response at that location and a large in-plane response at the sixth bearing near the third coupling.

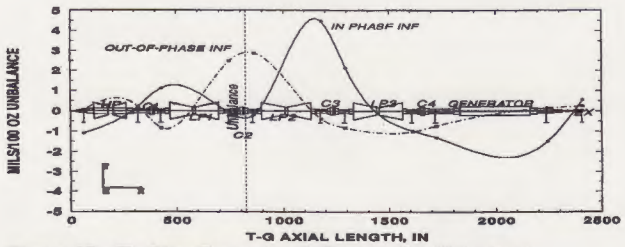

Figure 17 - Turbine-Generator Influence Coefficients at 1,800 RPM Due to Coupling No. 2 Unbalance

Figure 18 represents the in-plane and out-of-plane influence coefficients generated by a trial weight placed at coupling No. 3. There is a large response at coupling No. 2 due to the trial weight placed at coupling No. 3. Note that the in-plane components of the response due to

and 33.5 oz. at 102° on the steam end of the LP3 rotor.

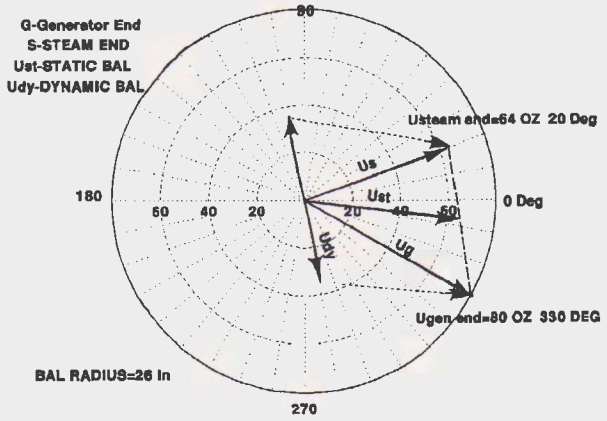

Figure 22 - Resolution of LP3 Turbine Balance Weights into Static and Dynamic Components

The computer program ***ROTORBAL-PC*** was used to predict the rotor response due to the static unbalance of 64 oz. at 353°. The influence coefficients as shown in Figure 20 were used to perform the calculations. Using these values of predicted amplitude, it was then possible to compute the response of the rotor to a pure dynamic or couple balance set for the LP3 rotor. Figure 23 represents the computed response of the turbine-generator due to a couple unbalance on the LP3 turbine. Note the large response of the LP3 couple on the generator response. It is apparent that high generator response may be controlled by dynamic balance shots placed on the LP3 turbine.

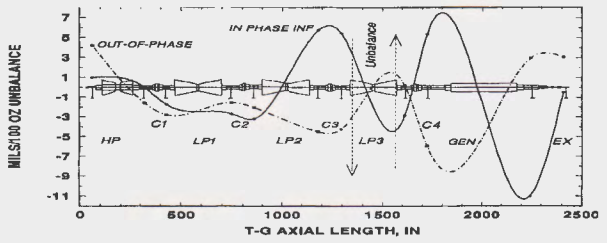

Figure 23 - Turbine-Generator Influence Coefficients at 1,800 RPM Due to LP3 Dynamic Unbalance

Table 2 represents a summary table of the influence coefficients for the turbine-generator for 100 oz. of unbalance per plane.

5 Multi-Plane Balancing of Turbine Generator

The influence coefficients for the various coupling balance planes and the LP3 turbine static and dynamic balancing coefficients are shown in Table 2. The response is shown in mils of amplitude per 100 oz. of unbalance at the various locations. These coefficients were used to generate the space curves as shown in the previous figures.

By means of the influence coefficients, various balancing predictions were generated using the couplings by themselves and the addition of the couplings and a dynamic couple on the LP3 turbine. Table 3 represents various multi-plane balancing corrections generated for three planes of coupling, five planes using a dynamic balance on LP3, and six planes of balancing using the theoretical influence coefficients generated for the first coupling. Table 4 represents the initial amplitude and the final amplitude predicted with three, five, and six planes of balancing. In the first balance prediction, using couplings 2, 3, and 4, it was found that the rotor amplitude would increase at bearing locations 1, 3, 7, and 11. The increase in amplitude at these locations is shown with a plus. It is therefore apparent that with only three coupling locations used for a simultaneous balance, eight of the bearing amplitudes reduce, while three become larger. For example, the amplitude at probe 3 has increased to 5.25 mils. Also, it is desirable that the amplitude does not exceed 3 mils at the exciter. The amplitude at the exciter, after the three coupling balance shots have been added, has increased to 3.42 mils, as shown in Table 4.

In the second balancing calculation, two planes on the LP3 turbine were used in addition to the three coupling locations. Although five physical planes are used in the balancing, from a computer standpoint this is a four-plane balance prediction, since a dynamic couple placed at the LP3 turbine is treated as one balancing entity. By applying the dynamic couple at the LP3 turbine, it is seen that all planes have been improved in amplitude. There has been a considerable reduction in the amplitude at bearing 3 from 5.25 to 2.16 mils. Also, the amplitude at the exciter is less than 3 mils. However, with the five planes of balancing, it is not possible to reduce all levels of vibration below 3 mils. For example, bearings 4, 5, and 8 have amplitudes above 3 mils.

In the six-plane balancing calculations, the first coupling location was used in addition to the other planes. The influence coefficients generated for the first coupling location are based on theoretical predictions. Therefore, the calculations of the balance weights for these cases cannot be actually applied to the rotor until the actual influence coefficients for the No. 1 coupling are determined experimentally. However, this computation does illustrate the improvement in the overall balancing by employing the No. 1 coupling for additional balancing. In the first six-plane balance

calculation, no weighting was applied to any of the vibration measurements. One of the advantages of the multi-plane balancing ***ROTORBAL-PC*** program is the ability to emphasize particular amplitudes of vibration for the purpose of balancing. In the first balancing calculation with six planes, all vibration readings were treated with equal emphasis. In this case, very low levels of amplitude were obtained at bearings 1, 3, 5, 6, and 7. However, the amplitude at the bearing 8 is 3.56 mils and the exciter has increased to 3.89 mils. This is considered to be undesirable. In the second six-plane calculations, weighting functions were employed at probes 3, 4, 8, and 11. The weighting function of .8 was used at bearing No. 3. This allowed the amplitude to increase. A weighting function of 1.5 was used at bearings 4, 8, and 11. The final theoretical six-plane balancing prediction demonstrates that the amplitude at all levels can be reduced below 3 mils.

6 Summary and Conclusions on Multi-Plane Turbine Generator Balancing

The following are concepts of multi-plane balancing that have been developed from the computation of the theoretical rotor dynamical response and from the application of Unit No. 2 turbine-generator measured influence coefficients from various balancing runs.

1. The four coupling locations are inadequate to balance the entire turbine-generator system. This is because the turbine-generator operates through at least ten modes, so four balancing planes are insufficient.

2. The rotor will require at least six to seven simultaneous planes of balancing to reduce the vibrations at all probes below 3 mils.

3. Low-speed balancing of the individual turbines and generator on a balancing machine is recommended to balance out the rotor mass centers. The first five critical speeds encountered by the turbine-generator system are essentially excitations due to the mass centers of the various LP, HP, and generator rotors. By properly balancing the rotors on a balancing machine, the vibration of the lower modes will be minimized.

4. After the rotor passes through the first five critical speeds, the turbine and generator rotor mass centers become node points. This means that the mass centers have very little motion and most of the amplitude of a particular turbine component is a conical motion in which the ends are out of phase. No attempt should be made to place balancing weights at the turbine rotor centers to balance out amplitude at running speed, as this will cause excessive motion at the lower critical speeds.

5. The use of static balancing components on the turbines at running speed is to be discouraged. A static balancing distribution is one in which the weights are placed in phase on the two ends of the turbine. This is equivalent to adding mass center unbalance. This balancing weight distribution can cause an extremely large turbine response when passing through the lower turbine-generator critical speeds. The resulting rotor response can be large enough to cause bowing of the turbine rotors.

6. A dynamic couple placed on the LP rotors can have a significant effect on controlling amplitude of the LP rotors, as well as the generator at running speed. Dynamic couples for balancing at running speed are encouraged, rather than the use of static balance components. A dynamic balancing set is one in which two equal weights are placed out of phase on opposite ends of the turbine. This weight distribution will cause a minimal response at the lower turbine-generator critical speeds, which are mainly driven by mass center imbalance. Generator amplitude can also be controlled by means of dynamic or couple balance weights on the LP rotors without having to specifically balance the generator. Field balancing of a generator is to be avoided.

7. The influence coefficients due to a pure dynamic couple on the LP3 rotors can be been computed based on static and quasi-dynamic balancing shots placed on the LP3 rotor. The balancing combination of the dynamic set on the LP3 along with three coupling balance weights will reduce the overall vibration levels. This represents five simultaneous planes of balance correction.

8. The least squared error based RODYN computer program, ***ROTORBAL-PC***, may be used to predict multi-plane balancing corrections based on the combination of the various influence coefficients generated from the coupling balance runs and the LP3 balance runs.

9. Influence coefficients should be developed for both no-load and fully-loaded conditions. This is equivalent to using two speed cases in the balancing program. Substantial changes in the balancing influence coefficients can occur under full power operation. Vibration data taken at different power levels should not be mixed.

10. The number one coupling and the exciter location

Table 2 - Experimental Influence Coefficients for SONGS Unit No. 2
(Units — Mils/100 oz. Unbalance)

Probe	Probe Location	Balance Location									
		Coupling No. 2		Coupling No. 3		Coupling No. 4		LP3 Static		LP3 Dynamic	
		Mag	Phase	Mag	Phase	Mag	Phase	Mag	Phase	Mag	Phase
1	HPs	1.1	177°	1.9	124°	0.8	114°	2.3	29°	4.3	77°
2	HPg	0.3	43°	1.6	317°	0.5	213°	1.8	229°	1.6	270°
3	LP1s	1.4	323°	2.8	261°	1.7	158°	7.8	130°	3.3	238°
4	LP1g	2.5	92°	3.6	45°	2.6	315°	1.7	17°	3.1	210°
5	LP2s	2.9	94°	4.5	9°	2.8	330°	0.6	295°	3.8	213°
6	LP2g	4.5	355°	4.8	144°	3.3	61°	3.7	94°	7.3	322°

Table 3 - Multi-Plane Balancing Corrections

No. of Planes	Coupling No. 1*		Coupling No. 2		Coupling No. 3		Coupling No. 4		$LP3_s$		$LP3_g$	
	W, oz.	Phase	W, oz.	Phase	W, oz.	Phase	W, oz.	Phase	W, oz.	Phase	W, oz.	Phase
3			77.3	95°	32.7	341°	17	268°				
5			125	98°	109	351°	46	314°	68	124°	68	304°
6	164	358°	108	113°	79	17°	30	315°	40	148°	40	328°
6**	154	93°	86	12°	56	308°	55	307°	86	162°	86	342°

* Based on theoretically developed influence coefficients for coupling No. 1 unbalance
** Probe weighting on 3, 4, 8, and 11

Table 4 - Initial and Predicted Rotor Response with Coupling Planes and LP3 Dynamic Couple Balancing

Probe Location	Initial	3-Planes CPLS 2, 3, & 4	5 Planes CPLS 2, 3, 4, & LP3 Dynamic	6 Planes* CPLS 1–4, & LP3 Dynamic	
1	2.17	2.37 (+)	1.68	**0.8**	.92 **
2	1.77	1.55	**1.17**	1.83	1.98
3	4.87	5.25 (+)	2.16	**1.20**	2.98
4	5.45	**4.3**	3.56	3.87	**2.83**
5	4.21	3.6	3.87	**0.69**	.86
6	3.55	1.0	2.57	**0.91**	1.13
7	2.27	2.99 (+)	1.35	**0.72**	2.09
8	4.26	**2.15**	3.26	3.56	2.62
9	3.47	**1.48**	2.55	1.95	2.32
10	2.19	1.12	2.15	0.89	**.62**
11	2.97	3.42 (+)	**2.77**	3.89 (+)	**2.77**

* Based on theoretical coupling No. 1 influence coefficients
Bold = lowest amplitude
** Probe weighting factors on 3, 4, 8, & 11

can be used to provide additional planes of balance. Actual system influence coefficients should be generated for these locations.

11. The change in turbine-generator rotor response due to either changes in coupling balance or unbalance in the LP3 rotor may be predicted from the measured turbine-generator influence coefficients using the RODYN balancing program.

Bibliography on Rotor Balancing

Badgley, R. H., 1974, "Recent Developments in MultiPlane Multispeed Balancing of Flexible Rotors in the United States," International Union of Theoretical and Applied Mechanics, Lyngby, Denmark.

"*CRITSPD-PC* User's Manual," RODYN Vibration Analysis, Inc., Charlottesville, VA.

Darlow, M., 1989, "Flexible Rotor Balancing by the Unified Balancing Approach," Rensselaer Polytechnic Institute, Troy, N.Y.

Foiles, W., and E. J. Gunter, 1982, "Balancing a Three Mass Rotor with Shaft Bow," University of Virginia, Charlottesville.

Goodman, T. P., 1964, "A Least-Squares Method for Computing Balance Corrections," Journal of Engineering for Industry, 86(3): 273–279.

Gunter, E. J., Z. Fang, and J. R. Henderson, 1994, "Static and Dynamic Analysis of a 1150 MW Turbine-Generator System, Part I: Static Analysis,"Vibration Institute Proceedings, 18th Annual Meeting, June 21–23, pp. 41–54

Gunter, E. J., and R. Humphris, 1986, "Field Balancing of 70 MW Gas Turbine-Generators," Proceedings of International Conference on Rotordynamics, ASME, (Tokyo), pp. 135–143.

Gunter, E., and C. Jackson, "Balancing of Rigid and Flexible Rotors," Chapter 3, Handbook of Rotor Dynamics, McGraw, Hill, 1992

Gunter, E. J., H. Springer, and H. H. Humphris, 1982, "Balancing of a Multimass Flexible Rotor-Bearing System Without Phase Instruments," Proceedings of Conference on Rotordynamics Problems in Power Plants, Rome, Italy, September.

Jackson, C., 1979, "Practical Vibration Primer," Gulf Publishing Co., Houston, TX.

Kellenberger, W., 1972, "Should a Flexible Rotor Be Balanced in N or (N+2) Planes?" Journal of Engineering for Industry, 94: 548–560.

Lund, J. W., and J. Tonnesen, 1972, "Analysis and Experiments on Multi-Plane Balancing of Flexible Rotors," Journal of Engineering for Industry, 94(1): 233.

Mechanalysis, Inc., "Vector Calculations for Two Plane Balancing," Applications Report 327, IRD, Columbus, Ohio.

"*MSC/Pal2* Users Manual Ver. 4.0," The MacNeal-Schwendler Corporation, Los Angeles, CA.

Nicholas, J. C., E. J. Gunter, and P. E. Allaire, 1976, "Effect of Residual Shaft Bow on Unbalance Response and Balancing of a Single Mass Flexible Rotor: Part I - Unbalance Response; Part II - Balancing," Journal of Engineering for Power, 98(2): 171–189.

Palazzolo, A. B., and E. J. Gunter, 1977, "Multimass Flexible Rotor Balancing by the Least Squares Error Method," Vibration Institute, Clarendon Hills, Ill.

Rieger, N., 1986, "Balancing of Rigid and Flexible Rotors," SVN 12, The Shock and Vibration Center.

"*ROTORBAL-PC* User's Manual," RODYN Vibration Analysis, Inc., Charlottesville, VA.

Schenek Trebel Corp., 1980, "Fundamentals of Balancing," Deer Park, Long Island, New York.

Technical Information Letter 1012-2, August 1987, "Effect of Electrical System Variations on Turbine-Generator Torsional Response," General Electric Company, Schenectady, N.Y.

Tessarik, J. M., 1970, "Flexible Rotor Balancing by the Exact Point-Speed and Least Squares Procedure for Flexible Rotor Balancing by the influence coefficient Method," ASME 73-DET-115, New York.

Thearle, E. L., 1934, "Dynamic Balancing of Rotating Machinery in the Field," Transactions of ASME, 56: 745–753.